View metadata, citation and similar papers at core.ac.uk
brought to you by CORE
provided by Elsevier - Publisher Connector

Cell Reports
Resource
Open ACCESS

Disease-Association Analysis of an Inflammation-Related Feedback Loop

Masaaki Murakami,[1,7,*] Masaya Harada,[1,7] Daisuke Kamimura,[1,7] Hideki Ogura,[1] Yuko Okuyama,[1] Noriko Kumai,[1] Azusa Okuyama,[1] Rajeev Singh,[1] Jing-Jing Jiang,[1] Toru Atsumi,[1] Sayaka Shiraya,[1] Yuji Nakatsuji,[2] Makoto Kinoshita,[2] Hitoshi Kohsaka,[4] Makoto Nishida,[6] Saburo Sakoda,[5] Nobuyuki Miyasaka,[4] Keiko Yamaguchi-Takihara,[6] and Toshio Hirano[3,*]

[1]Laboratory of Developmental Immunology, JST-CREST, Graduate School of Frontier Biosciences, Graduate School of Medicine, and WPI Immunology Frontier Research Center
[2]Department of Neurology, Graduate School of Medicine
[3]JST-CREST
Osaka University, Osaka 565-0871, Japan
[4]Department of Medicine and Rheumatology, GCOE Program, International Research Center for Molecular Science in Tooth and Bone Diseases, Graduate School of Medical and Dental Sciences, Tokyo Medical and Dental University, Tokyo 113-8519, Japan
[5]Department of Neurology, National Hospital Organization Toneyama Hospital, Osaka 560-0045, Japan
[6]Health Care Center, Osaka University, Osaka 560-0043, Japan
[7]These authors contributed equally to this work
*Correspondence: murakami@molonc.med.osaka-u.ac.jp (M.M.), hirano@molonc.med.osaka-u.ac.jp (T.H.)
http://dx.doi.org/10.1016/j.celrep.2013.01.028

SUMMARY

The IL-6-triggered positive feedback loop for NFκB signaling (or the IL-6 amplifier/Inflammation amplifier) was originally discovered as a synergistic-activation signal that follows IL-17/IL-6 stimulation in nonimmune cells. Subsequent results from animal models have shown that the amplifier is activated by stimulation of NFκB and STAT3 and induces chemokines and inflammation via an NFκB loop. However, its role in human diseases is unclear. Here, we combined two genome-wide mouse screens with SNP-based disease association studies, revealing 1,700 genes related to the IL-6 amplifier, 202 of which showed 492 indications of association with ailments beyond autoimmune diseases. We followed up on ErbB1 from our list. Blocking ErbB1 signaling suppressed the IL-6 amplifier, whereas the expression of epiregulin, an ErbB1 ligand, was higher in patients with inflammatory diseases. These results indicate that the IL-6 amplifier is indeed associated with human diseases and disorders and that the identified genes may make for potential therapeutic targets.

INTRODUCTION

IL-6 is thought to have an important role in the development of autoimmune diseases and other inflammatory conditions (Awasthi and Kuchroo, 2009; Hirano, 1998, 2010; Nishihara et al., 2007; O'Shea et al., 2002; Sakaguchi and Sakaguchi, 2005). It is also one of the many cytokines induced by $CD4^+$ T cells. In addition, IL-6 is required for the development of Th17 cells, which are IL-17-expressing activated $CD4^+$ T cells (Bettelli et al., 2007; Cua et al., 2003; Harrington et al., 2005; Park et al., 2005; Veldhoen et al., 2006) that are strongly correlated with various autoimmune models (Afzali et al., 2007; Bettelli et al., 2007; Hirota et al., 2007; Iwakura and Ishigame, 2006; Ogura et al., 2008). IL-6 signaling has been studied in various inflammatory disease models including F759 mice, which express a mutant variant of the IL-6 signaling transducer gp130, which enhances STAT3 activation due to deficient SOCS3-mediated negative feedback (Ohtani et al., 2000). As these mice age, they spontaneously develop an MHC class II-associated, IL-6-dependent, tissue-specific joint disease (F759 arthritis) that resembles rheumatoid arthritis (Atsumi et al., 2002; Sawa et al., 2006). Furthermore, the development of F759 arthritis is mediated by the excessive activation of IL-6 signaling in nonimmune, IL-7-expressing tissue, which causes development of Th17 cells (Hirano, 2010; Ogura et al., 2008; Sawa et al., 2006), suggesting that the interaction between nonimmune tissue and immune system plays a crucial role in some autoimmune diseases.

We identified the IL-6 amplifier/Inflammation amplifier as a positive feedback loop for NFκB targets, including IL-6, in type 1 collagen$^+$ cells after stimulation with IL-17 and IL-6 (Ogura et al., 2008). The amplifier is induced by simultaneous activation of NFκB and STAT3 and acts as a local chemokine inducer to cause inflammation via a NFκB loop. Indeed, the IL-6 amplifier is important for the development of autoimmune disease in F759 arthritis and EAE, a multiple sclerosis model (Arima et al., 2012; Murakami and Hirano, 2011; Murakami et al., 2011; Ogura et al., 2008). Here, we considered whether the IL-6 amplifier/Inflammation amplifier is also associated with human disease.

Recent advances in mammalian RNAi and small hairpin RNA (shRNA) technologies have made it possible to screen systematically for phenotypes that indicate inactive intracellular signaling. We systemically screened, using an shRNA system

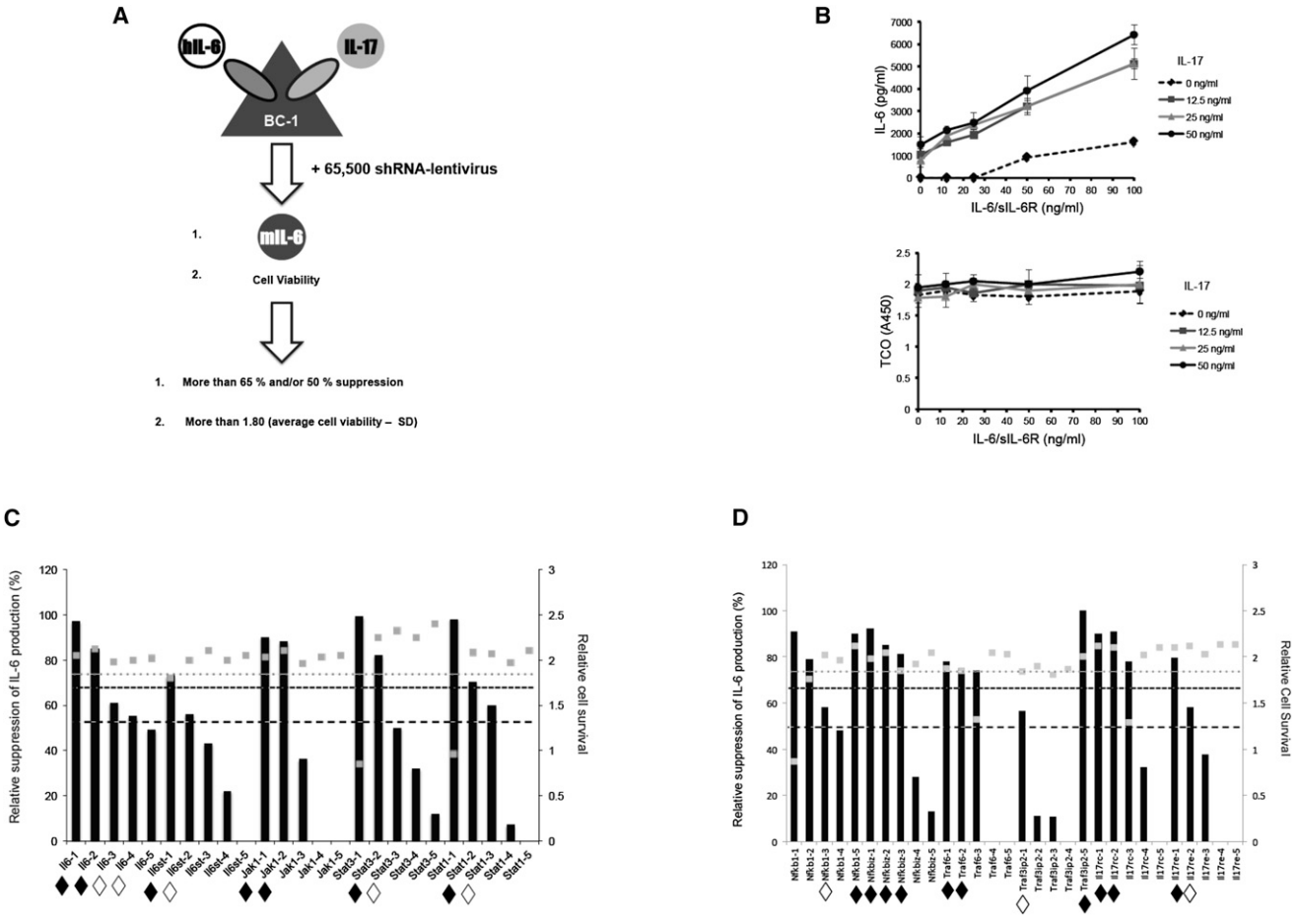

Figure 1. Scheme for Screening Positive Regulators of IL-6-Mediated Amplification and Inflammation

(A) Schematic of the primary screen. A BC1 mouse type 1 collagen$^+$ cell line was cultured in 96-well plates and treated with a lentivirus that encoded shRNA specific for candidate genes. The resulting BC1 cells were stimulated with human IL-6, soluble IL-6 receptor, and mouse IL-17. Mouse IL-6 concentrations in the supernatant and cell survival were measured by ELISA and mitochondrial activity, respectively.

(B) Top: Mouse IL-6 expression in BC1 cells stimulated with various concentrations of human IL-6, human soluble IL-6 receptor, and mouse IL-17. Bottom: Survival of BC1 cells transduced with control shRNA after stimulation with various concentrations of human IL-6, human soluble IL-6 receptor, and mouse IL-17.

(C and D) Candidate genes were selected based on two criteria: (i) expression of mouse IL-6, and (ii) cell survival. We selected shRNA that resulted in mouse IL-6 expression levels that were less than 35% the average IL-6 expression level in the 96-well plate. Cell survival was also evaluated based on mitochondrial activity using TCO reagent (gray squares). The mean and SD for all BC1 cells were 1.88 and 0.08, respectively. The threshold value was therefore set at 1.88 − 0.08 = 1.8. shRNA-screening results specific for 11 known genes in the IL-6 (C) and IL-17 (D) signaling pathways are shown. Mouse IL-6 expression levels are represented by the black bars; relative cell survival by the gray squares. Black and white diamonds on the bottom denote shRNA that fulfilled the primary screening criteria by more than 65% and inhibited IL-6 production by more than 50%, respectively. Dashed lines indicate thresholds (65%, 50%, and 1.8).

See also Figures S1, S2, S3, S4, S5, S6, and Table S10.

and DNA microarray, for regulators and/or targets of IL-6 amplifier activation and, thus, identify genes critical for chronic inflammation. Because animal models do not always apply to human diseases and disorders, we also considered SNP analysis (Lander, 2011). Recent genome-wide association studies (GWASs) have successfully associated SNPs with an individual susceptibility to various pathologies. As a result, we attempted to establish an approach that combines two methods, systemic screening and GWAS, to identify which genes may potentially regulate the development of human diseases and disorders via inflammation, finding that the IL-6 amplifier/Inflammation amplifier is associated with a number of diseases and disorders beyond autoimmune ones.

RESULTS

In-Vitro High-Throughput Functional Screening of Candidate Genes Involved in IL-6 Amplifier Activation

We first sought to identify which genes positively regulate IL-6 amplifier activation. To do this, we used a lentivirus expression system to perform a genome-wide shRNA screen in BC1 murine type 1 collagen$^+$ cells. The expression of IL-6, which is also synergistically induced by IL-6 and IL-17 (Ogura et al., 2008), was used as a readout for the shRNA screen (Figure 1A). BC1 cells were stimulated with human IL-6 plus soluble IL-6 receptor and IL-17. The expression level of mouse IL-6 and cell viability were measured (Figure 1B).

We tested about 65,500 lentivirus lines encoding shRNA, which corresponds to approximately 16,000 mouse open reading frames. We eliminated shRNA samples in which the cell survival appeared impaired by using a threshold value defined as the mean of the mitochondrial activity (cell viability) for each shRNA minus one SD (1.88 − 0.08 = 1.80) because their reduced IL-6 levels may have been the result of low cell numbers in each well (see Experimental Procedures).

We then ranked candidate genes using the suppression rates for IL-6 production. We selected the ranking system based on the content rate of known signaling genes for the IL-6 and IL-17 pathways. We selected the system described below, which led to the inclusion of 11 known signaling genes for IL-6 and IL-17 pathways into the candidate list (Figures 1C and 1D). In the first selection (genes ranked 0 in Tables S1 and S2, third column from the left), at least three shRNAs of each gene suppressed over 65% of IL-6 production. In the second selection (those ranked 1), two shRNAs suppressed over 65%, and in the third selection (those ranked 2), one shRNA suppressed over 65%, and at least one other shRNA suppressed 50%. We did not select genes that had at least two shRNA lentiviruses with less than a −400% suppression in IL-6 expression regardless of the other selection criteria (see cells in second row from the right side of Table S3). The screening identified a total of 1,289 candidate genes as positive regulators for the amplifier (Table S2). Detailed data on the inhibition of IL-6 production by a specific shRNA as well as cell viability are listed in Table S3.

We also considered the genes for which only one shRNA had an inhibition rate >80% because this cutoff might be a good candidate. This list contains 1,670 genes, and 425 overlap with 1,289 candidates (Table S4). Because 1,670 genes contained less numbers of signaling genes for IL-6 and IL-17 pathways (data not shown), we investigated the 1,289 candidates here. However, we should not discard the genes that only one shRNA had worked because experiments using MEF cells isolated from mice without some of these genes showed that the gene-deficient cells suppress IL-6 expression after IL-6 and IL-17 stimulation (data not shown).

We performed a second screen using 27 randomly selected genes from those ranked 0–2. We established corresponding gene-deficient BC1 cells using 54 shRNAs (2 per gene) and stimulated them with IL-6 and/or IL-17. The shRNAs used here were the same as those in the first screen. Although more than 90% of shRNAs showed a statistically significant reduction (red numbers in Table S5), 23 and 10 of the 54 randomly selected shRNAs had an effect of more than 65% and 50%–65% suppression (see cells with an asterisk [*] in third column of Table S5), respectively, in response to IL-6 and IL-17. Thus, we estimate the false-positive rate in this genome-wide screening to be less than 40% (38.9%, 33 out of 54).

Moreover, we analyzed the mRNA expressions of two NFκB targets, *Il-6* and *Cxcl1*, both of which are hyperinduced after IL-17 stimulation particularly in the presence of IL-6 stimulation, and a STAT3 target, *Socs3*, which is induced by IL-6 stimulation, by using shRNA for 25 genes (*Gzmm* and *Pou4f1* were excluded from the list of 27 because *Gzmm* shRNA #3 did not inhibit IL-6 expression after IL-6 and IL-17 stimulation, and *Pou4f1* expression was too low to be detected by the real-time PCR detection system.) (Figures S1, S2, S3, S4, S5, and S6C; Table S5). We showed that at least one of the NFκB targets, *Il-6* or *Il-6* plus *Cxcl1*, was significantly suppressed in all 50 gene-deficient cells, whereas *Socs3* was suppressed in only 25 gene-deficient cells (Figures S1, S2, S3, S4, S5, and S6C). We validated the screening results using nine genes for 27 siRNA target sequences (3 siRNA/gene) that were different from the shRNA sequence. We selected the nine most suppressed siRNAs for the target mRNA expression and found that six out of nine (66.6%) significantly suppressed *Il-6* mRNA expression after IL-6 and IL-17 stimulation (Table S5). Thus, consistent with the shRNA second screening results (Table S5), we also suggested the false-positive rate in this genome-wide screening to be less than 40%. These results suggest that the false-positive rate in our first screen was relatively low. Therefore, at least half of the 1,289 candidate genes identified in functional screening should be involved in IL-6 amplifier activation. However, only three out of nine siRNAs in Table S5 suppressed *Il-6* mRNA by more than 50%, which is the cutoff in the first shRNA screening, which was obtained from IL-6 ELISA. Although we hypothesize that the knockdown efficiency of each target protein might vary due to protein stability because of a transient effect of siRNA, it might be possible that the false-positive rate of the shRNA screen may be higher. Thus, we might need to give attention to the overlapped gene lists, which obtain from combined results between differential genome-wide screenings described below.

We compared the data of these 1,289 genes with those of more than 1,000 randomly selected genes (see "randomly selected control set (1,097)" in Table 1) to investigate whether certain pathways and/or molecular characteristics are significantly enriched in our list. The ingenuity systems pathway analysis (IPA)-based analysis demonstrated that only genes related to pathways such as immune response and unclassified were significantly enriched, whereas genes known to be related to multiple biological processes were also present in the shRNA list but insignificantly enriched (Tables 1 and S2). Thus, activation of the IL-6 amplifier appears to be affected by multiple biological processes and regulated by many genes.

Relationships between Candidate Genes that Are Positive Regulators for IL-6 Amplifier Activation and Human Diseases and Disorders

Among the 1,289 candidate genes, 1,177 have human homologs (see blank cells in the column "mouse alone" of Table S2). Using the Genetic Association Database (GAD) and two GWAS papers by Consortium (2007) and Johnson and O'Donnell (2009), we next investigated disease associations. We selected a total of 33 diseases and disorders including 8 autoimmune diseases, 3 metabolic syndromes, 6 neurodegenerative diseases, 4 psychotic illnesses, and 12 other inflammatory diseases, finding 140 genes combined for a total of 334 positive associations (Tables 2 and S1).

We then performed statistical comparison analysis using the results of the functional shRNA screen and the control group of more than 10,000 randomly selected genes (see the row "Mouse shRNA control" in Table 2). The number of expected disease associations per gene including the control group is shown in the column "Expected Disease Association" of Table 2.

Table 1. Summary of Biological Processes and Cellular Localizations and Functions of the Candidate Genes for IL-6 Amplifier-Positive Regulators, IL-6 Amplifier Targets in Mouse, and IL-6 Amplifier Targets in Human

	Biological Processes											Cellular Localizations and Functions											
	Immune Response	Development	Transport	Signal Transduction	Cell Cycle	Apoptosis	Adhesion and Cell Movement	Metabolic Process	Others	Unclassified	Sum	Extracellular Space	Plasma Membrane	Receptor Activity	Receptor Binding	GPCR	Transporter	Channel	Enzyme	Kinase Related	Mitochondria	Nucleus	Others or Unknown	Sum
Randomly selected control set (1097)	51	213	181	190	71	94	65	243	251	145	1504	58	247	116	50	38	56	40	348	98	55	337	383	1826
Mouse shRNA screening	77	211	235	228	66	121	85	206	323	209	1761	76	287	147	63	33	75	37	289	100	82	306	365	1860
p values	0.076	0.026	0.133	0.407	0.079	0.244	0.251	0.000	0.108	0.020		0.260	0.442	0.260	0.353	0.098	0.223	0.143	0.000	0.150	0.079	0.000	0.000	
Mouse DNA array	57	111	67	90	34	74	36	120	140	71	800	55	142	55	50	13	28	9	181	56	14	183	133	919
p values	0.000	0.472	0.000	0.323	0.324	0.003	0.130	0.267	0.257	0.303		0.001	0.163	0.256	0.000	0.086	0.414	0.008	0.450	0.298	0.006	0.330	0.000	
Human DNA array	69	165	112	133	65	105	36	156	195	177	1213	64	171	65	56	5	30	16	269	45	27	298	257	1303
p values	0.002	0.332	0.008	0.085	0.223	0.008	0.000	0.006	0.327	0.000		0.037	0.042	0.007	0.041	0.000	0.031	0.007	0.263	0.001	0.015	0.081	0.003	
Mouse and human DNA array overlap	18	16	13	21	7	16	6	20	12	6	135	13	25	6	11	0	5	1	31	8	3	29	12	144
p values	0.000	0.408	0.353	0.055	0.285	0.001	0.357	0.429	0.025	0.045		0.000	0.092	0.139	0.001	0.039	0.397	0.110	0.226	0.472	0.258	0.306	0.000	

First, second, fourth, sixth, and eighth lines show gene numbers of the indicated pathway, molecular characteristics, and molecular localization in control, mouse shRNA screening, mouse DNA microarray, human DNA microarray, and mouse and human DNA array overlaps, respectively. Third, fifth, seventh, and ninth lines show p values for gene enrichment in mouse shRNA screening, mouse DNA microarray, human DNA microarray, and mouse and human DNA array overlaps, respectively, when compared with over 1,000 control genes ("control (1,097 genes)"). Red-colored numbers indicate statistically significant increases, whereas those with blue numbers show statistically significant decreases ($p < 0.1$). See also Tables S3, S4, S5, and S10.

Four of the five disease categories (all but psychotic illnesses) were significantly enriched in the gene list (see Table 2, summary). More specifically, genes relating to six autoimmune diseases (rheumatoid arthritis, multiple sclerosis, celiac disease, lupus, pancreatitis, and thyroiditis/Grave's disease), three metabolic syndromes (cardiovascular diseases/atherosclerosis/systemic sclerosis, hypertension/blood pressure, and type 2 diabetes/NIDDM), four neurodegenerative diseases (Alzheimer's disease/hippocampal atrophy, neuropathy, ALS, and prion disease), and nine other inflammatory diseases (atopy/dermatitis/allergy, pulmonary disease/asthma/cystic fibrosis, hepatitis, inflammatory bowel disease/colitis, vitiligo, periodontitis, polyposis, stroke, and nephropathy/glomerulonephritis) were significantly enriched (Table 2). These results strongly suggest that the candidate genes positively involved in IL-6 amplifier activation are critical for the development of many human diseases and disorders.

Relationships between Candidate Genes Induced after IL-6 Amplifier Activation and Human Diseases and Disorders

We hypothesized that target genes of the IL-6 amplifier could also associate with various human diseases and disorders. We employed microarray analysis to study these genes in type 1 collagen$^+$ fibroblasts with or without IL-6 and IL-17 stimulation (Table S6). We selected 576 target genes after performing the experiment twice (Table S7) and ranked them based on their increased level of expression 12 hr after stimulation (ranking 0–2 third column in Table S7). Indeed, among the 576 candidate genes, 542 have human homologs (see blank cells in the fourth column of Table S7). IPA-based analysis with over 1,000 randomly selected control genes showed that genes related to some pathways such as immune response, apoptosis, and molecular characteristics such as extracellular space and receptor binding were significantly enriched in the mouse microarray list (Tables 1 and S7).

GAD identified 70 of the 542 genes to have 202 positive associations with various diseases and disorders (Tables 2 and S8). We then performed statistical comparison analysis using these results and the control set of over 10,000 randomly selected genes (see the row "Mouse DNA array control" in Table 2). The same four disease categories from the shRNA screening results were significantly enriched in the microarray gene list (Table 2). Moreover, genes related to six autoimmune diseases (type 1 diabetes/IDDM, Crohn's disease, rheumatoid arthritis, lupus, pancreatitis, and thryoiditis/Grave's disease), three metabolic syndromes (cardiovascular diseases/atherosclerosis/systemic sclerosis, hypertension/blood pressure, and type 2 diabetes/NIDDM), two neurodegenerative diseases (Alzheimer's disease/hippocampal atrophy and Parkinson's disease), and seven other inflammatory diseases (pulmonary disease/asthma/cystic fibrosis, hepatitis, inflammatory bowel disease/colitis, sepsis, psoriasis/scleroderma, stroke, and nephropathy/glomerulonephritis) were significantly enriched (Table 2).

We showed that human type 1 collagen$^+$ cell lines synergistically express *Il-6* after IL-6 and IL-17 stimulation (Figure S7A). We employed human microarray analysis to study the target genes directly in a human type 1 collagen$^+$ synovial fibroblast line with or without IL-6 and IL-17 stimulation. We selected 885 target gene candidates after performing the experiment twice (Table S9) and ranked them based on their increased level of expression 12 hr after stimulation (ranking 0–2, third column in Table S7). IPA-based analysis with over 1,000 randomly selected control genes showed that genes related to pathways such as

Table 2. Summary of Associations between Human Diseases and Disorders and Candidate Genes for IL-6 Amplifier-Positive Regulators and for IL-6 Amplifier Targets in Mouse and Human Systems

	Number Of Selected Genes	Number Of Disease Associations	Expected Disease Associations	Autoimmune Diseases								Metabolic Syndromes			Neurodegenerative Diseases						Psychotic Illnesses				Other Inflammatory Diseases									Summary					
				Type 1 Diabetes/IDDM	Crohn's Disease	Rheumatoid Arthritis	Multiple Sclerosis	Celiac Disease	Lupus	Pancreatitis	Thyroiditis/Grave's Disease	Cardiovascular Diseases/ Atherosclerosis/Systemic Sclerosis	Hypertension/Blood Pressure	Type 2 Diabetes/NIDDM	Alzheimer's Disease/Hippocampal Atrophy	Parkinson's Disease	Neuropathy	Amyotropic Lateral Sclerosis	Prion Disease	Epilepsy	Schizophrenia	Bipolar Disorder	Depression	Cognitive Performance	atopy/Dermatitis/Allergy	Pulmonary Disease/Asthma/Cystic Fibrosis	Hepatitis	Inflammatory Bowel Disease/Colitis	Sepsis	Vitiligo	Periodontitis	Polyposis	Psoriasis/Scleroderma	Stroke	Nephropathy/Glomerulonephritis	GVHD/Transplantation Complication	Autoimmune Diseases	Metabolic Syndrome	Neurodegenerative Diseases	Psychotic Illnesses	Other Inflammatory Diseases
Mouse shRNA screening	1177	334	0.284	13	7	15	17	8	17	4	5	33	25	27	16	4	2	6	1	1	16	5	7	2	12	28	9	9	2	5	7	2	4	7	16	2	86	85	30	30	103
Mouse shRNA control	12226	1813	0.148	105	60	86	64	45	67	10	24	168	187	211	108	61	0	16	0	10	125	43	48	35	33	128	3	45	17	3	22	0	35	21	27	10	461	566	195	251	344
p values			0.000	0.195	0.315	0.015	0.000	0.052	0.000	0.004	0.054	0.000	0.059	0.080	0.052	0.227	0.000	0.001	0.001	0.486	0.140	0.344	0.150	0.234	0.000	0.000	0.000	0.020	0.394	0.000	0.002	0.000	0.372	0.001	0.009	0.167	0.000	0.000	0.007	0.128	0.000
Mouse DNA array	542	202	0.373	14	10	11	5	3	9	2	4	23	18	20	8	6	0	1	0	0	5	3	2	1	3	19	5	5	3	0	2	0	6	5	8	1	58	61	15	11	57
Mouse DNA array control	11694	1814	0.155	99	57	86	63	41	70	11	23	172	185	203	107	55	2	18	1	10	127	45	48	29	40	127	8	42	15	7	25	2	32	23	31	12	450	560	193	249	364
p values			0.000	0.000	0.000	0.000	0.120	0.220	0.001	0.027	0.004	0.000	0.001	0.000	0.093	0.020	0.381	0.430	0.415	0.248	0.360	0.270	0.441	0.385	0.208	0.000	0.000	0.019	0.006	0.285	0.226	0.381	0.000	0.000	0.000	0.009	0.284	0.000	0.000	0.025	0.438	0.000
Human DNA array	885	265	0.299	12	9	15	8	10	12	4	6	33	14	22	15	5	0	1	0	2	7	2	2	4	7	20	7	12	4	2	3	0	11	6	6	4	109	69	23	15	82
Human DNA array control	11715	1772	0.151	92	55	82	66	40	67	10	21	174	187	198	99	54	2	18	1	11	122	45	46	33	37	122	8	42	16	8	22	2	29	20	35	8	433	559	185	246	349
p values			0.000	0.035	0.014	0.001	0.000	0.000	0.002	0.001	0.001	0.000	0.487	0.041	0.005	0.331	0.349	0.382	0.392	0.119	0.238	0.229	0.219	0.184	0.011	0.000	0.000	0.000	0.012	0.054	0.165	0.349	0.000	0.001	0.028	0.000	0.000	0.000	0.000	0.011	0.208	0.000
Mouse and Human array overlap	87	71	0.816	4	3	3	3	2	3	1	1	9	4	7	3	3	0	0	0	0	1	1	0	0	1	5	5	2	1	0	0	0	2	3	3	1	20	20	6	2	23
Array overlap control	11743	1937	0.165	107	64	94	65	42	76	12	26	183	197	213	110	58	2	19	1	10	131	47	51	30	43	140	8	45	18	7	27	2	36	26	35	12	486	593	200	259	399
p values			0.000	0.000	0.000	0.003	0.000	0.002	0.001	0.002	0.035	0.000	0.018	0.005	0.008	0.000	0.452	0.354	0.466	0.393	0.488	0.137	0.269	0.319	0.116	0.000	0.000	0.002	0.010	0.410	0.327	0.452	0.001	0.000	0.000	0.002	0.000	0.000	0.000	0.000	0.477	0.000

The first, fourth, seventh, and tenth lines show the number and percentage of genes with indicated disease/disorder associations based on the GAD website for our mouse shRNA screening, mouse DNA microarray, human DNA microarray, and mouse and human DNA array overlaps, respectively. The 3rd, 6th, 9th, and 12th lines show p values for gene enrichment in the mouse shRNA screening, mouse DNA microarray, human DNA microarray, and mouse and human DNA array overlaps, respectively, when compared with over 10,000 control genes. Red numbers indicate statistical differences ($p < 0.1$). See also Tables S1, S2, S3, S4, S5, and S10.

immune response, apoptosis, and unclassified, molecular characteristics such as extracellular space and receptor binding, and nucleus were significantly enriched in the human microarray list (Tables 1 and S7). GAD identified 94 of the 885 genes as having 265 positive associations with various diseases and disorders (Tables 2 and S8). We then performed statistical comparison analysis using these results and the control set of over 10,000 randomly selected genes (see the row "Human DNA array control" in Table 2). Once again, the same four disease categories were significantly enriched in the human microarray gene list (Table 2). Moreover, genes related to eight autoimmune diseases (type 1 diabetes/IDDM, Crohn's disease, rheumatoid arthritis, multiple sclerosis, celiac disease, lupus, pancreatitis, and thryoiditis/Grave's disease), two metabolic syndromes (cardiovascular diseases/atherosclerosis/systemic sclerosis and type 2 diabetes/NIDDM), one neurodegenerative disease (Alzheimer's disease/hippocampal atrophy), and ten other inflammatory diseases (atopy/dermatitis/allergy, pulmonary disease/asthma/cystic fibrosis, hepatitis, inflammatory bowel disease/colitis, sepsis, vitiligo, psoriasis/scleroderma, stroke, nephropathy/glomerulonephritis, and GVHD/transplantation complications) were significantly enriched (Tables 2 and S8). Thus, we confirmed the involvement of the IL-6 amplifier in the development of many human diseases and disorders by human microarray experiments.

Additionally, in the microarray studies, we found 87 overlaps between the 542 mouse and 885 human targets and 16 overlaps between the 70 mouse and 94 human genes associated with human diseases. We performed IPA-based analysis of the 87 genes with over 1,000 randomly selected control genes and showed that the genes among them related to the pathways, immune response, signal transduction, apoptosis, and molecular characteristics such as extracellular space, plasma membrane, and receptor binding were significantly enriched (Tables 1 and S7). GAD identified 16 of the 87 genes as having 71 positive associations with various diseases and disorders (Tables 2 and S8). We then performed statistical comparison analysis using these results and the control set of over 10,000 randomly selected genes (see the row "Array overlap control" in Table 2). Once again, the aforementioned four disease categories were significantly enriched in the overlaps (Tables 2 and S8). Moreover, genes related to eight autoimmune diseases (type 1 diabetes/IDDM, Crohn's disease, rheumatoid arthritis, multiple sclerosis, celiac disease, lupus, pancreatitis, and thryoiditis/Grave's disease), three metabolic syndromes (cardiovascular diseases/atherosclerosis/systemic sclerosis, hypertension/blood pressure, and type 2 diabetes/NIDDM), two neurodegenerative diseases (Alzheimer's disease/hippocampal atrophy and Parkinson's disease), and eight other inflammatory diseases (pulmonary disease/asthma/cystic fibrosis, hepatitis, inflammatory bowel disease/colitis, sepsis, psoriasis/scleroderma, stroke, nephropathy/glomerulonephritis, and GVHD/transplantation complications) were significantly enriched (Tables 2 and S8). We hypothesize that these overlaps might be critical for the development of diseases and disorders via IL-6 amplifier activation.

The Epiregulin-ErbB1 Pathway Plays a Role in IL-6 Amplifier Activation

To further establish the importance of the amplifier activation in human diseases and disorders, we sought to select specific

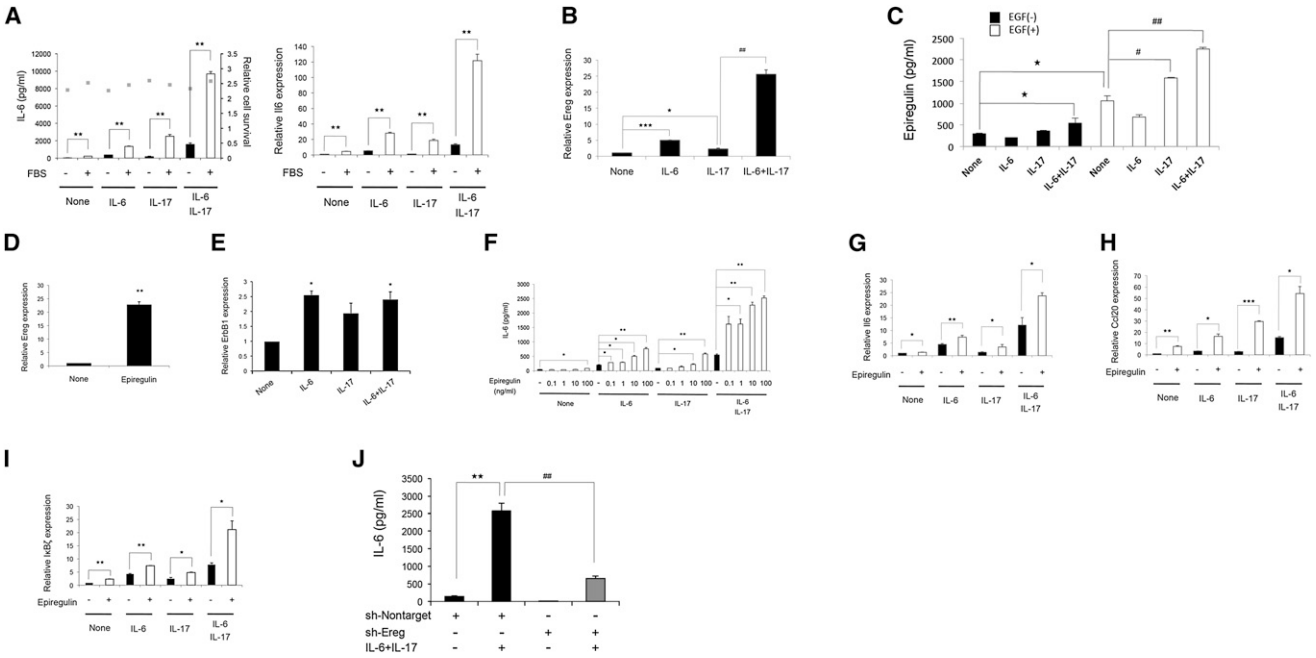

Figure 2. The Epiregulin-ErbB1 Pathway Activates the IL-6 Amplifier In Vitro

(A) IL-6 amplifier activation was suppressed in the absence of FBS. BC1 cells were stimulated with human IL-6 plus soluble IL-6 receptor and/or IL-17 for 24 hr in the absence or presence of 10% FBS. Gray dots indicate cell survival values monitored by TCO reagent. Left: Culture supernatants were collected and assessed using an ELISA specific for mouse IL-6. Cell survival was also evaluated based on mitochondrial activity (gray squares; all points were above the threshold value). Right: *Il-6* mRNA expression 3 hr after stimulation was evaluated using real-time PCR.

(B) BC1 cells were stimulated with human IL-6 plus soluble IL-6 receptor and/or IL-17 in the absence of FBS for 3 hr. Epiregulin (*Ereg*) expression was then evaluated using real-time PCR.

(C) BC1 cells were stimulated with human IL-6 plus soluble IL-6 receptor and/or IL-17 in the absence of FBS for 48 hr with or without EGF, another ErbB1 ligand. Culture supernatants were collected and assessed using an ELISA specific for epiregulin.

(D) BC1 cells were stimulated with epiregulin in the absence of FBS for 3 hr. Epiregulin (*Ereg*) expression was evaluated using real-time PCR.

(E) BC1 cells were stimulated with human IL-6 plus soluble IL-6 receptor and/or IL-17 in the absence of FBS for 3 hr. *ErbB1* (*Egfr*) expression was then evaluated using real-time PCR.

(F) BC1 cells were stimulated with human IL-6 plus soluble IL-6 receptor and/or IL-17 in the absence of FBS for 24 hr with or without various concentrations of epiregulin. Culture supernatants were collected and assessed using ELISA specific for IL-6.

(G–I) *Il-6* (G), *Ccl20* (H), and *IκBζ* (I) mRNA expressions in BC1 cells 3 hr (G and H) or 1 hr (I) after stimulation with human IL-6 plus soluble IL-6 receptor and/or IL-17 in the absence of FBS with or without epiregulin were evaluated using real-time PCR.

(J) BC1 cells were treated with a lentivirus encoding shRNA specific for epiregulin (*Ereg*) and cultured in the presence of puromycin. The resulting cells were stimulated with human IL-6 plus soluble IL-6 receptor and/or IL-17 in the absence of FBS for 48 hr. Culture supernatants were collected and assessed using ELISA specific for mouse IL-6.

Mean scores ± SD are shown. p values were calculated using Student's t tests. * and #, $p < 0.05$; ** and ##, $p < 0.01$; ***$p < 0.001$.

See also Figure S7 and Table S10.

molecules from the aforementioned genes. We targeted the ErbB1 pathway because (i) soluble molecule concentrations are relatively easy to measure; (ii) ErbB1 and its ligands associate with diseases and disorders like SLE, asthma, and cardiovascular diseases; and (iii) ErbB1 is included in the eight overlapping genes that are associated with human diseases and disorders and found in the both our shRNA screen and mouse DNA array lists.

We then investigated IL-6 expression in the absence of fetal bovine serum (FBS), a rich source of ErbB1 ligands. Indeed, IL-6 expression was significantly reduced in these cultures despite stimulation with IL-6 and/or IL-17 (Figure 2A). Epiregulin, an ErbB1 ligand, was synergistically expressed after IL-6 and IL-17 stimulation, particularly in the presence of EGF (Figures 2B, 2C, and S7). Furthermore, *Ereg* (that encodes epiregulin) mRNA expression was induced in the presence of epiregulin (Figures 2D and S7C), and IL-6 stimulation increased *ErbB1* (*Egfr*) expression (Figure 2E). Importantly, epiregulin enhanced the expression of IL-6 and other targets after IL-6 and IL-17 stimulation (Figures 2F–2I and S7), whereas *Ereg* deficiency by shRNA decreased it (Figure 2J; data not shown). Thus, we concluded that an epiregulin-ErbB1 pathway is involved in IL-6 amplifier activation.

It is important to understand how the epiregulin pathway affects NFκB and/or STAT3 signaling. The phosphorylations of Akt, p65, and ERK1/ERK2 increased after epiregulin stimulation in the presence of IL-6 and IL-17 (Figure 3A). NFκB reporter activity also increased after epiregulin stimulation (Figure 3B), whereas a PI3K inhibitor, LY294002, but not a MEK inhibitor, suppressed it (Figure 3C; data not shown), suggesting that epiregulin enhances the PI3K-NFκB pathway. Consistent with

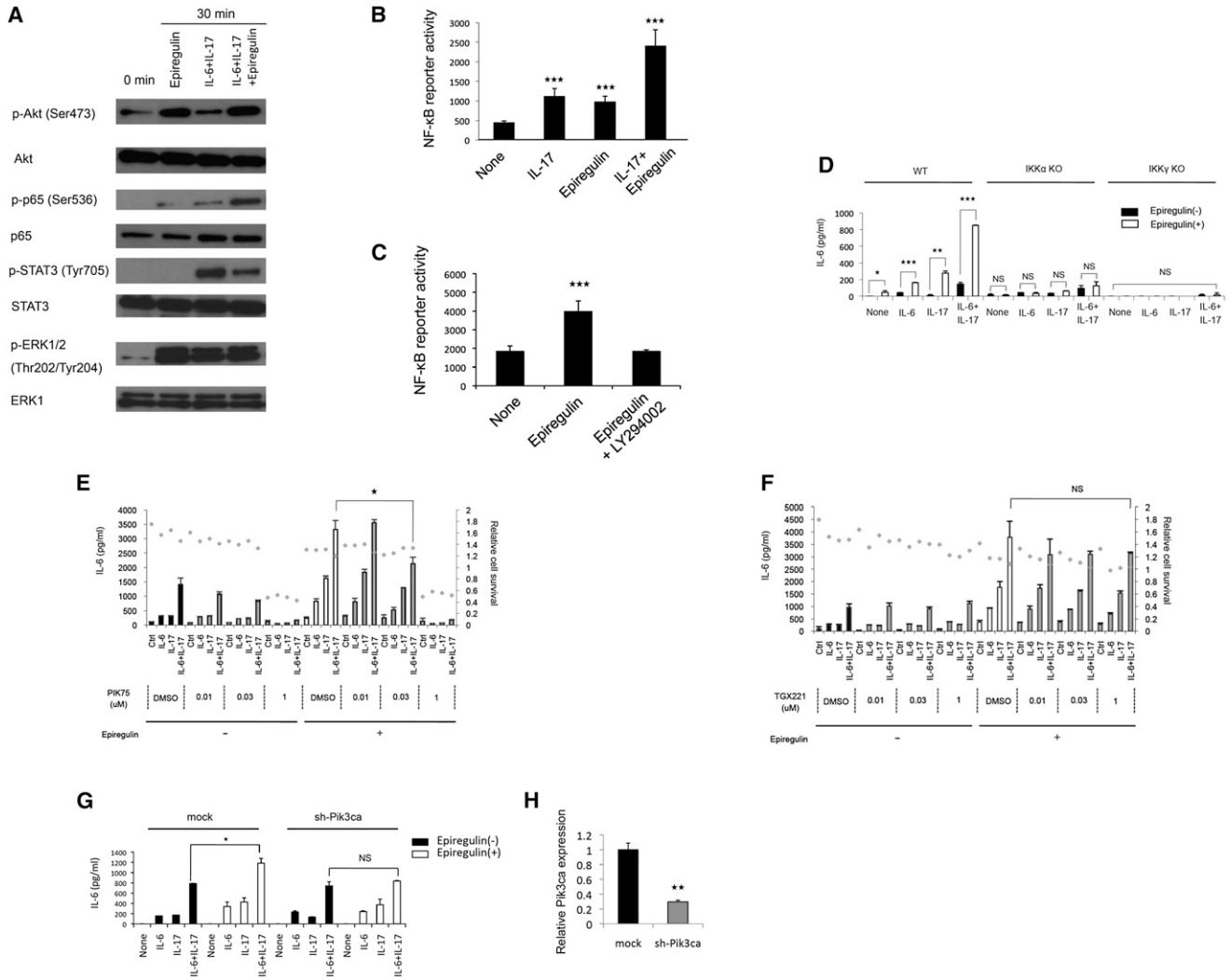

Figure 3. The Epiregulin Signal Enhances NFκB Activation via the PI3K α Pathway

(A) MEF cells were stimulated with epiregulin in the presence or absence of IL-6 and IL-17 and then investigated for the phosphorylation of Akt, p65, STAT3, and ERK1/ERK2.

(B) HeLa cells were stimulated with epiregulin in the presence or absence of IL-17 and then investigated for NFκB reporter activity using a 5× NFκB-luc construct.

(C) BC1 cells were stimulated with epiregulin in the presence or absence of LY294002 and then investigated for NFκB reporter activity using a 5× NFκB-luc construct.

(D) IKKα- and IKKγ-deficient MEF cells as well as wild-type MEF cells (WT) were stimulated with epiregulin (100 ng/ml) in the presence or absence of human IL-6 plus soluble IL-6 receptor and/or IL-17 for 12 hr. Culture supernatants were collected and assessed using an ELISA specific for mouse IL-6.

(E and F) BC1 cells were stimulated with human IL-6 plus soluble IL-6 receptor and/or IL-17 in the absence of FBS with or without epiregulin and various concentrations of PIK75 (E) or TGX221 (F) for 24 hr. Cell survival was also evaluated based on mitochondrial activity. Culture supernatants were collected and assessed using an ELISA specific for mouse IL-6.

(G and H) (G) BC1 cells were treated with a lentivirus encoding shRNA specific for *Pik3ca* and stimulated with epiregulin (100 ng/ml) in the presence or absence of human IL-6 plus soluble IL-6 receptor and/or IL-17 in the absence of FBS for 24 hr. Culture supernatants were collected and assessed using an ELISA specific for mouse IL-6. (H) *Pik3ca* expression was also evaluated using real-time PCR.

Mean scores ± SD are shown. p Values were calculated using Student's t tests. *$p < 0.05$; **$p < 0.01$; ***$p < 0.001$; NS, not significant.

See also Figure S9 and Table S10.

this, deficiencies in IKKα or IKKγ as well as a PI3K α inhibitor diminished the epiregulin-mediated enhancement, whereas a PI3K β inhibitor did not (Figures 3D–3F). Additionally, a deficiency of PI3K α suppressed the epiregulin-mediated enhancement of IL-6 expression (Figures 3G and 3H). Thus, we show that the epiregulin signal enhances NFκB activation via the PI3K α pathway.

The Epiregulin-ErbB1 Pathway Has a Role in Autoimmune Disease Models

We have shown that F759 arthritis is mediated nonhemopoietically, particularly in type 1 collagen$^+$ cells based on bone marrow transplantation and a tissue-specific-deficient system (Murakami et al., 2011; Ogura et al., 2008; Sawa et al., 2006).

Direct joint injections of IL-6 and IL-17 with a minimum modification of hemopoietic cells induced arthritis within 2 weeks in a manner dependent on the amplifier (Murakami et al., 2011). Co-injection of a lentivirus encoding shRNA for *Stat3* or *Rela* (NFκB p65) in combination with IL-6 and IL-17 significantly suppressed the disease (Murakami et al., 2011). We employed this method and showed that joint injections of these cytokines induce *Ereg* as well as *Il-6* expression in the joints (Figure 4A). On the other hand, joint injections of lentiviruses having *Ereg*- or *ErbB1* (*Egfr*)-shRNA suppressed these expressions (Figure 4A) as well as the development of F759 arthritis (Figures 4B and 4C). Joint injections of an anti-epiregulin antibody or ErbB1 tyrosine kinase inhibitors also suppressed the development of F759 arthritis (Figures 4D–4G), a result confirmed by histology (Figure 4H). These results too suggest that the epiregulin-ErbB1 pathway is involved in the activation of the IL-6 amplifier, leading to cytokine-induced arthritis. Moreover, systemic administration of an ErbB1 tyrosine kinase inhibitor significantly suppressed the development of EAE (Figure 4I) and decreased the number of infiltrating cells in the spinal cord (Figure 4J). Together, these results support the idea that the epiregulin-ErbB1 pathway contributes to the pathogenesis of autoimmune disease models most likely via the IL-6 amplifier.

Possible Epiregulin-ErbB1 Pathway Involvement in Human IL-6 Amplifier Activation

Human type 1 collagen$^+$ cells (Igarashi et al., 2010) also showed enhanced expression of IL-6 after IL-6 and IL-17 treatment. Additionally, epiregulin increased *Il-6* expression in the presence of IL-6 and IL-17, whereas an ErbB1 inhibitor suppressed it (Figures 5A and 5B). *Ereg* was synergistically expressed in human cells in response to IL-6 and IL-17 or itself (Figure 5C). These results demonstrate that epiregulin contributes to the amplifier activation in human cells in vitro.

We then evaluated whether epiregulin concentrations were elevated in patients with rheumatoid arthritis, atherosclerosis, and multiple sclerosis. Serum from patients suffering from one of these diseases contained higher concentrations of epiregulin compared to control subjects (Figures 5D–5F), consistent with epiregulin being involved in inflammatory diseases in mice through activation of the amplifier. Additionally, IL-6 concentrations increased in serum from patients suffering from these diseases (Figure S8; data not shown). These results too suggest that the epiregulin-ErbB1 pathway contributes to the activation of the IL-6 amplifier and has a role in the pathogenesis of various human diseases and disorders.

DISCUSSION

Using two mouse genome-wide screens, we here identified about 1,700 genes with human homologs that have a role in IL-6 amplifier/Inflammation amplifier activation or intensity. Because (1) many known IL-6 and IL-17 pathway positive regulators were selected in the shRNA screen list, (2) there was high reproducibility between the first and second functional screenings, (3) of the low false-positive rates in the functional screening, and (4) of the resemblances of the disease association patterns between the shRNA screening and the DNA microarray screenings (humans and mice), we concluded that our genome-wide screening systems were sound. Following comparisons with GWAS results, we found that among the 1,700 screened genes, 202 genes (140 from the shRNA screen and 70 genes from the DNA microarray analysis; with the following 8 genes overlapping: *ErbB1* [*Egfr*], *Il-6*, *Pde4b*, *Ptgs2*, *Serpine1*, *Slit2*, *Socs2*, and *Stat3*) showed over 490 indications of association not only with autoimmune diseases but also with metabolic syndromes, neurodegenerative diseases, and other inflammatory diseases. Furthermore, we showed that the epiregulin-ErbB1 pathway is involved in the development of autoimmune disease models. Moreover, the epiregulin-ErbB1 pathway enhanced the amplifier in human nonimmune cells, and the epiregulin concentration in serum was highest in patients with inflammatory diseases. These results suggest that IL-6 amplifier activation has an important role in human diseases and disorders by regulating chronic inflammation steps. Thus, we extended our previous conclusion about the IL-6 amplifier being critical to the development of chronic inflammation in mice to humans.

The IL-6 amplifier is a local chemokine inducer that induces inflammation via an accumulation of various immune cells. Therefore, it is reasonable that amplifier-related genes have many disease associations because inflammation is a general process that disturbs function in affected tissues. However, genes from psychotic illnesses were not significantly enriched in the IL-6 amplifier-related genes, which may indicate that they are relatively unaffected by inflammation. Strong associations were found between IL-6 amplifier-related genes and 12 diseases: rheumatoid arthritis, lupus, pancreatitis, thyroiditis/Grave's diseases, cardiovascular diseases/atherosclerosis/systemic sclerosis, type 2 diabetes/NIDDM, Alzheimer's disease/hippocampal atrophy, pulmonary disease/asthma/cystic fibrosis, hepatitis, inflammatory bowel disease/colitis, stroke, and nephropathy/glomerulonephritis (see Table 2). We propose that these 12 diseases could be candidates for the next clinical trial of blockers for IL-6 and IL-17. In fact, anti-IL-6R antibody has already been used against rheumatoid arthritis. Additionally, it is possible that the positive regulator candidates from the shRNA screen are involved in either the NFκB or STAT3 signaling pathways or both because the amplifier is a synergy between STAT3 and NFκB. Therefore, targets of the amplifier, which may act as inflammation regulators, could be potential therapeutic targets.

We found that several of the genes associated with human diseases in our screening lists are known to control NFκB or STAT3 activity. Such genes include *Cckbr* (Ferrand et al., 2005), *Ets1* (Thomas et al., 1997), *Irak1* (Song et al., 2006), *Pde4* (Schmitz et al., 2007), *Pla2g1b* (Jo et al., 2004), *Pou2af1* (Wolf et al., 1998), and *Zbp1* (Kaiser et al., 2008). Furthermore, we identified a number of genes that had previously unknown function to be necessary for NFκB- and/or STAT3-mediated signal transduction (data not shown). Interestingly, human disease-linked NFκB and/or STAT3-driven genes such as *Mthfr* (Pickell et al., 2005), *Ptgs2* (D'Acquisto et al., 1997; Kojima et al., 2000), and *Vegfa* (Adachi et al., 2006; Rojo et al., 2004) were required for IL-6 amplifier activation according to our functional screening, suggesting a possible positive feedback mechanism of IL-6 amplifier activation through these molecules. These

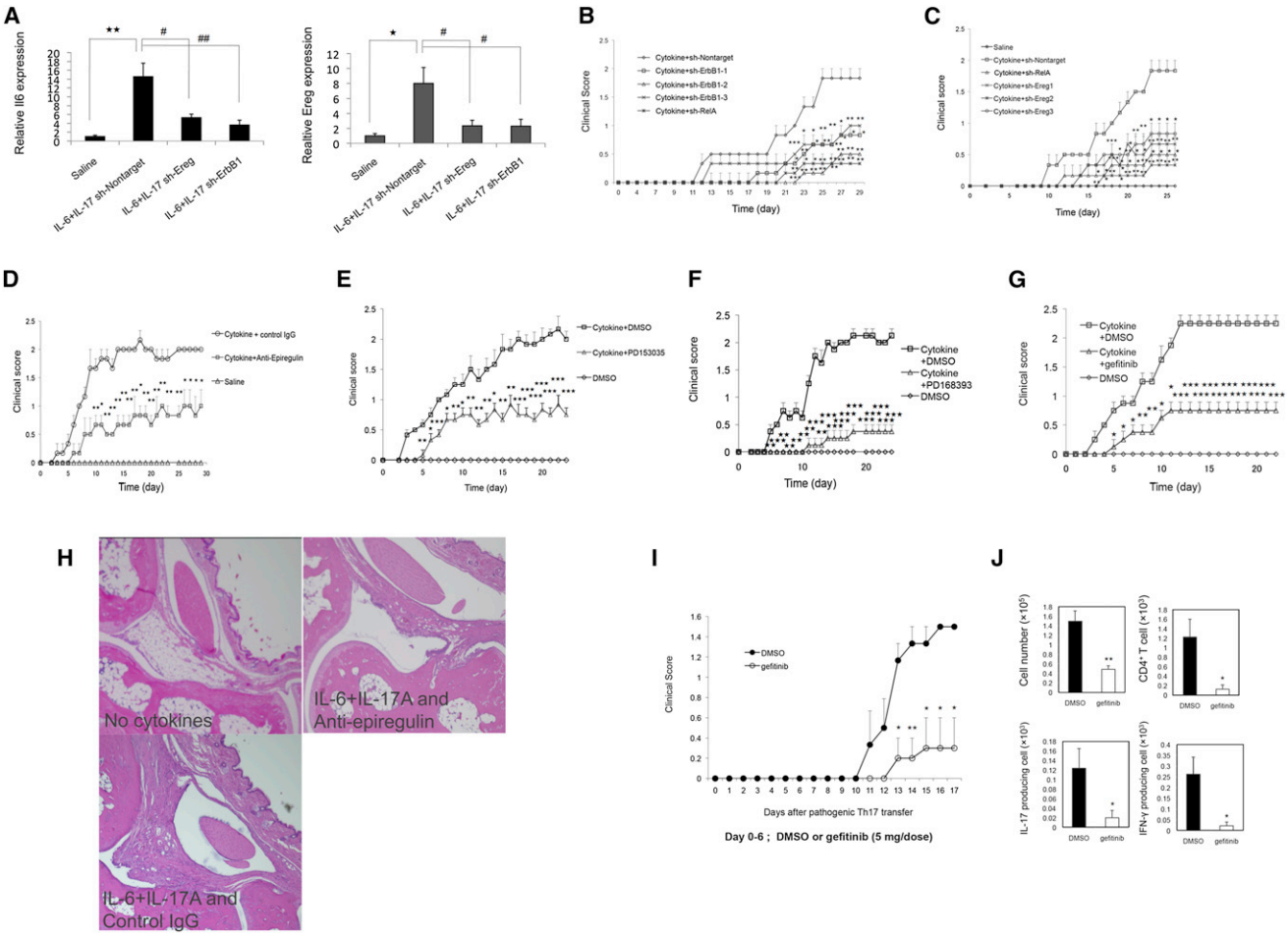

Figure 4. Epiregulin-ErbB1 Signaling Triggers Autoimmune Diseases in Mouse Models

(A) IL-6 and IL-17 on days 6, 7, and 8 were injected into the joints of F759 mice in the presence or absence of joint injections of lentivirus encoding shRNA specific for ErbB1 (*Egfr*) (n = 6), *Ereg* (n = 6), or a nontarget sequence (n = 6) on days 0, 2, and 4 followed by analysis of epiregulin and IL-6 expression in joint synovial tissues on day 15.

(B) Clinical arthritis scores from the left legs of F759 mice after left leg joint injections of 0.1 μg IL-17 and IL-6, respectively, on days 6, 7, and 8 and joint injections of lentivirus encoding shRNA specific for ErbB1 (*Egfr*) (open squares, open triangles, and crosses; n = 3), NFκB p65 (*Rela*) (asterisks; n = 3), or a nontarget sequence (diamonds; n = 3) on days 0, 2, and 4.

(C) Clinical arthritis scores from the left legs of F759 mice after left leg joint injections of 0.1 μg IL-17 and IL-6, respectively, on days 6, 7, and 8 and joint injections of a lentivirus encoding shRNA specific for epiregulin (*Ereg*) (crosses, asterisks, and open circles; n = 3), NFκB p65 (*Rela*) (open triangles; n = 3), or a nontarget sequence (squares; n = 3) on days 0, 2, and 4 and those from the left legs of F759 mice after left leg joint injections of saline alone (filled diamonds, n = 3).

(D) Clinical arthritis scores from the left legs of F759 mice after left leg joint injections of 0.1 μg IL-17 and IL-6, respectively, on days 0, 1, and 2 and joint injections of anti-epiregulin antibodies (1 μg) on days 0–23 (open squares, n = 3) and from the left legs of F759 mice after left leg joint injections of IL-17, IL-6, and control IgG (open circles, n = 3), or saline (open triangles, n = 3).

(E) Clinical arthritis scores from the left legs of F759 mice after left leg joint injections of 0.1 μg IL-17 and IL-6, respectively, on days 0, 1, and 2 and PD153035 (10 μg) on days 0–23 (triangles, n = 5) and from the left legs of F759 mice after left leg joint injections of IL-17, IL-6, and DMSO (squares, n = 5), or injections of DMSO only (diamonds, n = 5).

(F) Clinical arthritis scores from the left legs of F759 mice after left leg joint injections of 0.1 μg IL-17 and IL-6, respectively, on days 0, 1, and 2 and PD168393 (10 μg) on days 0–24 (triangles, n = 5) and from the left legs of F759 mice after left leg joint injections of IL-17, IL-6, and DMSO (squares, n = 5), or injections of DMSO only (diamonds, n = 5).

(G) Clinical arthritis scores from the left legs of F759 mice after left leg joint injections of 0.1 μg IL-17 and IL-6, respectively, on days 0, 1, and 2 and gefitinib (10 μg) on days 0–22 (triangles, n = 4) and from the left legs of F759 mice after left leg joint injections of IL-17, IL-6, and DMSO (squares, n = 4), or DMSO only (diamonds, n = 4).

(H) Ankle joints from each mouse in (D) were fixed and embedded in paraffin. Histological analysis was performed using sections stained with hematoxylin-eosin. These experiments were performed at least three times independently; representative data are shown.

(I) WT mice (2 months old) were intravenously injected with Th17 cells from WT mice with EAE and intraperitoneally injected with gefitinib (open squares, n = 5) or DMSO (open diamonds, n = 5) on days 0–6.

(J) WT mice (2 months old) were intravenously injected with Th17 cells from WT mice with EAE and intraperitoneally injected with gefitinib (closed bars, n = 5) or DMSO (open bars, n = 5) on days 0–6. Mononuclear cells from the spinal cords of Th17-transferred C57BL/6 mice were isolated on day 13. The resulting cell populations

(legend continued on next page)

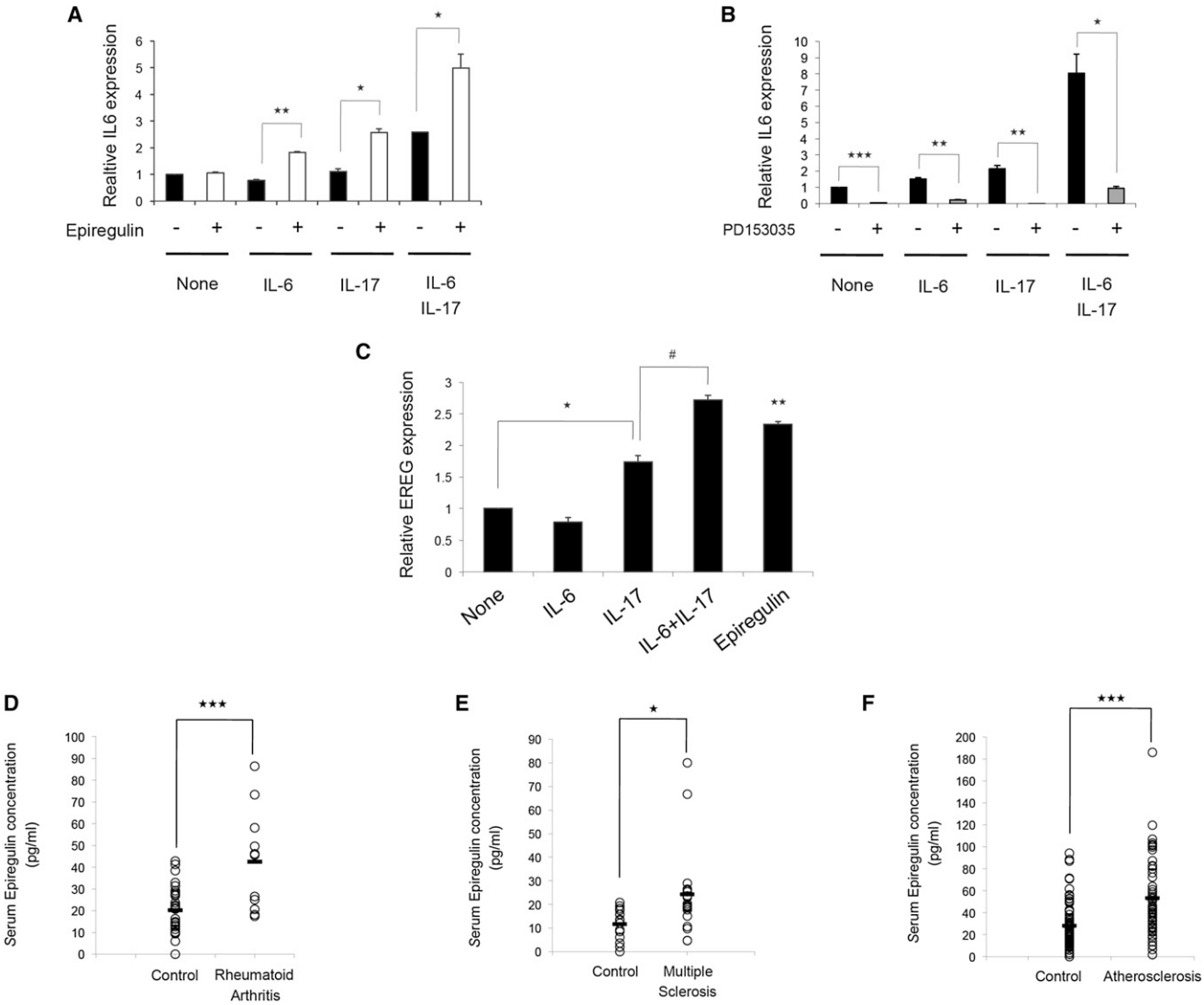

Figure 5. Epiregulin-ErbB1 Signaling Is Involved in Activation of the Human IL-6 Amplifier

(A) Human synovial cell lines were stimulated for 3 hr with human IL-6 plus soluble IL-6 receptor and/or IL-17 in the absence of FBS with or without epiregulin (100 ng/ml). *Il-6* expression in the resulting cells was evaluated using real-time PCR.

(B) Human synovial cells were stimulated for 3 hr with human IL-6 plus soluble IL-6 receptor and/or IL-17 in the presence of FBS with or without PD153035 (10 μg/ml). *Il-6* expression in the resulting cells was evaluated using real-time PCR.

(C) Human synovial cells were stimulated with human IL-6 plus soluble IL-6 receptor and/or IL-17 or epiregulin in the absence of FBS for 3 hr. *Ereg* expression in the resulting cells was evaluated using real-time PCR.

(D–F) Serum epiregulin concentrations in patients with (D) rheumatoid arthritis (n = 11), (E) atherosclerosis (n = 50), and (F) multiple sclerosis (n = 21) compared with healthy-aged, sex-matched subjects (rheumatoid arthritis, n = 26; atherosclerosis n = 64; multiple sclerosis, n = 15).

Mean scores ± SD are shown. p values were calculated using Student's t tests (* and #, $p < 0.05$; **$p < 0.01$; ***$p < 0.001$).

Related to Figures S7, S8, and Table S10.

results strengthen the significance of the synergy between NFκB and STAT3 molecules in human diseases and highlight the amplifier as a fundamental mechanism for enhancing inflammation through synergistic activation of these two critical transcription factors in nonimmune cells followed by a NFκB loop. We selected one gene, *ErbB1* (*Egfr*), from our gene list as a representative gene and analyzed its role in the development of inflammatory diseases. We demonstrated that NFκB activation via

were counted and stimulated in vitro with MOG peptide and bone marrow-derived dendritic cells. Twenty-four hours after in vitro stimulation, intracellular IL-17 and IFN-γ levels were examined. $CD4^+IL\text{-}17^+$ and $CD4^+IFN\text{-}\gamma$ T cells from Th17-transferred C57BL/6 mice treated with gefitinib or vehicle were counted. The number of $CD4^+IL\text{-}17^+$ and $CD4^+IFN\text{-}\gamma^+$ T cells in spinal cords was significantly lower in the recipients treated with gefitinib than in those treated with DMSO.

Mean scores ± SEM are shown. p Values were calculated using Student's t tests (* and #, $p < 0.05$; ** and ##, $p < 0.01$; ***$p < 0.001$). See also Table S10.

epiregulin-ErbB1 signaling is involved in the development of autoimmune diseases, and serum epiregulin concentrations increase in patients suffering from rheumatoid arthritis, multiple sclerosis, and atherosclerosis. Furthermore, we have identified over 30 genes from our genome-wide screening lists that are involved in the NFκB and/or STAT3 pathway and enhance IL-6 amplifier activation and the subsequent development of autoimmune diseases (data not shown). All these observations support the notion that the genes identified here are candidate regulators and/or targets of the IL-6 amplifier/Inflammation amplifier.

Curiously, *Il-4rα* and *Jak3* appeared in Table S3 because these are representative of IL-4. We confirmed via the second screening that deficiencies in *Il-4rα*, *Jak3*, and *Il-2rγ* (common γc) in BC1 cells significantly suppress IL-6 amplifier activation (Figure S9A). Furthermore, we showed that a certain amount of *Il-4* is expressed in BC1 cells and MEF cells even in steady state (Figure S9B). Therefore, we hypothesized that IL-4 signaling might also be involved in IL-6 amplifier activation.

Although positional cloning based on SNP analysis and genome-wide exome deep-sequencing studies have identified rare disease-causing mutations in several genes as the single most important risk factor for various complex diseases and disorders, recent GWAS analyses have identified numerous putatively susceptible loci that exert only very small risks (Manolio et al., 2009), meaning that a large proportion of the heritability of these diseases cannot be explained by current genome-wide analyses. It is likely that much of this "missing heritability" may be accounted for by multiple rare sequence variants and environmental factors including epigenetic effects (Hemminki et al., 2011; Manolio et al., 2009; Yang et al., 2010). Our results suggest that one missing heritability factor might be a preinflammatory milieu in the affected tissues, as has been suggested previously by Bertram et al. (2010), Kim et al. (2009), and Sewell et al. (2009). The accumulation of small functional alterations in such small risk variants in multiple effector genes including the candidate genes we identified here might result in activation networks for inflammation, particularly chronic inflammation, followed by the development of common diseases and disorders via local activation of the IL-6 amplifier. In other words, this might be one reason why many genes that regulate or are expressed after amplifier activation associate with many human diseases and disorders. Moreover, inflammation, particularly chronic inflammation, is a general event in many human diseases and disorders. Thus, the identified genes in this study, even those without clear SNP-based associations, may make for potential therapeutic targets against a number of human diseases.

In conclusion, this study may offer new clinical targets that can be used to impair the activation of the IL-6 amplifier in affected tissues. The approach described here enables rapid identification of relevant genes, many of which are likely involved in inducing the expression of chemokines, proinflammatory cytokines, and their regulators via IL-6-triggered NFκB feedback: IL-6 amplifier/Inflammation amplifier activation. Based on our genome-wide functional screen and comparisons with GWAS, we suggest the inhibition of the epiregulin-ErbB1 signaling pathway as a potential target for preventing amplifier activation and the subsequent development of inflammatory diseases and disorders. Future studies are needed to translate our results into effective treatments for patients with rheumatoid arthritis, atherosclerosis, multiple sclerosis, and many other diseases.

EXPERIMENTAL PROCEDURES

Mouse Strains

C57BL/6 mice were purchased from CLEA (Tokyo). The F759 mouse line, which carries a human gp130 variant (S710L), has been described previously (Atsumi et al., 2002). All mice were maintained under specific pathogen-free conditions according to protocols at the Osaka University Medical School. All animal experiments were performed following the guidelines of the Institutional Animal Care and Use Committees of the Graduate School of Frontier Biosciences and Graduate School of Medicine (Osaka University).

Clinical Assessment of Arthritis

Mice were inspected and assessed for signs of arthritis as described previously (Atsumi et al., 2002; Ishihara et al., 2004; Murakami et al., 2011; Ogura et al., 2008; Sawa et al., 2006). In brief, the severity of the arthritis was determined based on two bilaterally assessed parameters: (1) swelling in the ankle, and (2) restricted mobility of the ankle joints. The severity of each parameter was graded on a scale of 0–3, where 0 indicates no change; 1, mild change; 2, medium change; and 3, severe change. Averages for a single point in one leg ankle joint from each mouse were used.

Histological Analysis

Joints were fixed in 4% paraformaldehyde, decalcified for 12 hr in Morse's solution (22.5% bornyl formate and 10% sodium acid citrate solution), then 12 hr in 4% paraformaldehyde, and embedded in paraffin. Sections were stained with hematoxylin-eosin (Sawa et al., 2006).

Intracellular Cytokine Staining

The number of Th17 cells in vivo was determined as previously described by Nishihara et al. (2007). In brief, T cells from spleens were stimulated with phorbol myristate acetate and ionomycin (Sigma-Aldrich, Tokyo) in the presence of GolgiPlug (BD Biosciences, San Jose, CA, USA) for 6 hr. Intracellular IL-17 and IFN-γ were labeled with anti-IL-17 and anti-IFN-γ antibodies, respectively, after surface staining, fixation, and permeabilization.

Antibodies and Reagents

The following antibodies were used for flow cytometry analysis: APC-conjugated anti-IFN-γ (eBioscience, San Diego, CA) and control IgG1κ (eBioscience); FITC-conjugated anti-CD8 (eBioscience), anti-CD11b (Beckman Coulter, Brea, CA, USA), anti-CD11c (eBioscience), anti-CD19 (eBioscience), anti-NK1.1 (eBioscience), and anti-I-A/I-E (BioLegend, Tokyo); PE-conjugated anti-IL-17 (eBioscience), control IgG2a (eBioscience), and anti-I-A/I-E (BioLegend); and PE-Cy7-conjugated anti-CD4 (BioLegend). The following antibodies were used for western blotting: anti-phospho-p65 (Ser536, 93H1), anti-phospho-Akt (Ser473, 193H12), anti-phospho-STAT3 (Tyr705), anti-phospho-p44/p42 MAPK(Thr202/Tyr204, E10), anti-Akt, anti-STAT3 (all from Cell Signaling Technology, Danvers, MA, USA), anti-ERK1 (BD Bioscience), anti-p65 (C-20) (Santa Cruz Biotechnology, Santa Cruz, CA, USA), HRP-conjugated goat anti-rabbit IgG (H+L) (Southern Biotech, Birmingham, AL, USA), and HRP-conjugated goat anti-mouse IgG (H+L) (Invitrogen, Carlsbad, CA, USA). The following antibodies were used for in vivo neutralization: monoclonal anti-mouse epiregulin antibody (R&D Systems, Minneapolis) and purified rat IgG (Sigma-Aldrich).

The mission TRC shRNA library, shRNA clones, LPS, puromycin, polybrene, MOG peptide (33–55), Incomplete Freund's Adjuvant, protease inhibitor cocktail, and phosphatase inhibitor cocktail 2 were obtained from Sigma-Aldrich. TetraColor One reagent was purchased from Seikagaku (Tokyo). Mouse Epiregulin ELISA Kit, Human soluble IL-6 receptor α, mouse IL-23, human epiregulin, mouse epiregulin, and anti-mouse epiregulin antibody were obtained from (R&D Systems). Mouse and human IL-17 were obtained from PeproTech (Rocky Hill, NJ, USA). Human IL-6 was obtained from Toray Industries (Tokyo). PD153035, PD168393, LY294002, PIK75, and TGX221 were purchased from

Merck (Whitehouse Station, NJ, USA). Gefitinib (brand name, Iressa) was purchased from Tocris Bioscience (Minneapolis). Epiregulin and IL-6 concentrations in patients were measured by a detection kit purchased from Merck (Tokyo) or Bio-Rad (Tokyo) followed by analysis with a multiplex analysis device (Bio-Rad) or by ELISA kits (eBioscience).

A control shRNA lentivirus (GCGCGATAGCGCTAATAATTT) and undisclosed control siRNA were purchased from Sigma-Aldrich. The company claimed that the sequences were bioinformatically designed to not hit any transcripts in human, mouse, or rat genomes and that it functions in cells as expected. BC1 cells infected with a control shRNA lentivirus or a GFP lentivirus (Sigma-Aldrich) as well as BC1 cells without infection expressed comparable levels of IL-6 after cytokine stimulation (Figure S9C).

Cells and Stimulation Conditions

A type 1 collagen$^+$ endothelial BC1 cell line (Zhang et al., 1998) was obtained from Dr. M. Miyasaka (Osaka University). MEF cells were prepared from C57BL/6 fetuses (13–18 days postcoitus) as described previously by Sawa et al. (2006). MEF cells were sometimes immortalized via the transfection of SV40-T antigen. Synovial fibroblasts were prepared as described previously by Igarashi et al. (2010). HeLa cells were used in the reporter assay.

For stimulation, MEF cells were plated in 96-well plates (1×10^4 cells/well) and stimulated with human IL-6 (50 ng/ml; Toray Industries) plus human soluble IL-6 receptor (50 ng/ml; R&D Systems) and/or mouse IL-17 (50 ng/ml; R&D Systems) for 24 or 3 hr after 2 hr of serum starvation. Cell culture supernatant was collected for ELISAs. In some experiments, cells were harvested, and total RNA was prepared for real-time PCRs. Human synovial cell lines were obtained as described previously by Igarashi et al. (2010).

Genome-wide shRNA Screen

BC1 cells were harvested and counted using a cell counter. The cells were then cultured on day 1 in a 96-well flat-bottom plate (1,000 cells/well) in 100 μl of RPMI 1640 containing 10% FBS. The medium was replaced on day 2 with a RPMI 1640 containing lentivirus carrying candidate-specific shRNA (35 μl diluted 7×), 10% FBS, and 8 μg/ml polybrene. On day 3, 200 μl RPMI 1640 containing 10% FBS and 5 μg/ml puromycin was added to each well. On day 6, 100 μl RPMI 1640 containing 10% FBS, 100 ng/ml human IL-6, 100 ng/ml human soluble IL-6 receptor, and 50 ng/ml mIL-17 were added to each well. Supernatants were collected, and ELISAs for mouse IL-6 were performed. The resulting cells were evaluated for viability on day 7 using TetraColor One reagent.

Microarray Analysis

W26 cells and human synovial cells were stimulated with 100 ng/ml human IL-6, 100 ng/ml human soluble IL-6 receptor, and 50 ng/ml mIL-17 or hIL-17 for 3 or 12 hr. Total RNA isolated from the cells was processed into biotinylated cRNA, which was then hybridized to Affymetrix GeneChips (Tokyo). Raw data were processed with the MAS5 algorithm for probe-level normalization.

ELISA

IL-6 and epiregulin concentrations in cell culture supernatant were determined using ELISA kits (BD Bioscience, eBioscience, or R&D Systems).

Flow Cytometry

For cell surface labeling, 10^6 cells were incubated with fluorescence-conjugated antibodies for 30 min on ice. The cells then were analyzed with CyAn flow cytometers (Beckman Coulter). The collected data were analyzed using FlowJo software (Tree Star, Ashland, OR, USA).

Joint Injections

IL-17 (R&D Systems), IL-6 (Toray Industries), or saline was injected into the joints as described previously by Maffia et al. (2004). Joints were injected with a lentivirus carrying shRNA specific for *ErbB1* (*Egfr*), *Ereg*, and p65 (*Rela*) (Sigma-Aldrich), a lentivirus carrying a scrambled sequence (Sigma-Aldrich), or anti-epiregulin antibodies or ErbB1 inhibitors, as described previously by Maffia et al. (2004).

Real-Time PCRs

The 7300 Fast Real-Time PCR System (Applied Biosystems, Tokyo) and SYBR green PCR Master Mix (Sigma-Aldrich and KAPA Biosystems, Woburn, MA, USA) were used to quantify levels of target mRNA and *Hprt* mRNA. Total RNA was prepared from BC1 cells, MEF cells, and synovial tissues using a GenElute Mammalian Total RNA kit (Sigma-Aldrich) and DNase I (Sigma-Aldrich). The PCR primer pairs used are shown in Table S10. The conditions for real-time PCRs were 40 cycles at 94°C for 15 s followed by 40 cycles at 60°C for 60 s. The relative mRNA expression levels were normalized to the levels of *Hprt* or *Gapdh* mRNA.

Western Blotting

MEF cells were stimulated by the indicated cytokines and lysed with lysis buffer (20 mM Tris-HCl [pH 7.4], 150 mM NaCl, 1% Triton X-100, and 1mM EDTA) supplemented with protease inhibitor cocktail and phosphatase inhibitor cocktail 2 (Sigma-Aldrich). Five to 20 μg of total protein was run on 5%–20% SDS-PAGE (Wako, Tokyo). After transfer to a polyvinylidene fluoride membrane (Millipore, Billerica, MA, USA), immunoblotting was performed according to the manufacturer's protocol.

Luciferase Reporter Assay

A pGL4.32[*luc2P*/NF-κB-RE/Hygro] vector and pRL-TK vector were transiently cotransfected into HeLa cells and BC1 cells using FuGENE HD Transfection reagent (Promega, Tokyo). Cells were harvested 24 hr after transfection and stimulated with the indicated reagents for 5 hr. Luciferase activities of total cell lysates were measured using the Dual-Luciferase Reporter Assay System (Promega).

Induction of Th17 Cell Differentiation and EAE Development

EAE induction was performed as described previously (Arima et al., 2012; Ogura et al., 2008).

Mononuclear Cell Isolation from Spinal Cords

Mononuclear cells were isolated from spinal cords after cardiac perfusion with PBS, as described previously by Sawa et al. (2009).

Human Serum Preparations

Serum was collected from 11 patients with rheumatoid arthritis at Tokyo Medical and Dental University Hospital, 50 patients with atherosclerosis at Osaka University Health Care Center, and 21 patients with clinically defined multiple sclerosis (negative for autoantibody presence) at Osaka University Hospital. Serum was also collected from 64 healthy subjects at Osaka University Health Care Center. Informed consent was obtained from each patient. This study was approved by the Ethics Committees of Osaka University Hospital and Tokyo Medical and Dental University.

Bioinformatic Analysis

Bioinformatic analysis of the candidate genes in screening and the increased genes in DNA array analysis was done mainly using the GAD at the National Institute of Aging (http://geneticassociationdb.nih.gov/cgi-bin/index.cgi) for associations of human diseases and disorders, IPA and OMIM for gene characters, and IPA for network searching. We declared disease associations when the GAD reported "association/Yes," meaning the presence of statistically positive associations, or when the candidate gene was found to localize in a relevant chromosomal region based on data from two GWAS papers by Consortium (2007) and Johnson and O'Donnell (2009).

Statistical Analysis

Student's t tests (one or two tailed) were used for the statistical analyses of differences between groups. A p value of <0.1 was used as a cutoff for the bioinformatic results including Tables 1 and 2 but $p < 0.05$ for the biology experiments including Figures 1, 2, 3, 4, and 5.

SUPPLEMENTAL INFORMATION

Supplemental Information includes nine figures and ten tables and can be found with this article online at http://dx.doi.org/10.1016/j.celrep.2013.01.028.

LICENSING INFORMATION

This is an open-access article distributed under the terms of the Creative Commons Attribution License, which permits unrestricted use, distribution, and reproduction in any medium, provided the original author and source are credited.

ACKNOWLEDGMENTS

We thank Dr. Katsuhiko Ishihara (Kawasaki Medical University) for providing us critical information about the culturing of human type 1 collagen^{+} cells. We also thank Dr. Masatatsu Ogura (Hosei University) for providing us various critical statistical advices. We appreciate the excellent technical assistance provided by Ms. Eri Yoshimoto (Tokyo Medical and Dental University), and thank Ms. Ryoko Masuda (Osaka University) for her excellent secretarial assistance and Dr. Hideyuki Iwai for applying the Ethics Committees of Osaka University Hospital and Tokyo Medical and Dental University. We thank Dr. Peter Karagiannis (Osaka University) and Dr. Daniel W. Nebert (University of Cincinnati) for carefully reading the manuscript. We are grateful to Dr. Kenji Okonogi (Osaka University) for important suggestions on the data analyses of the screening results. We also thank Mr. Hironao Suzuki (Osaka University), Dr. Eri Sanda (Osaka University), and Dr. Chika Kitabayashi (Osaka University) for data entry of the genome-wide screening. This work was supported by KAKENHI (to M.H., D.K., H.O., M.M., and T.H.), the CREST Program of the Japan Science and Technology Agency (to T.H. and M.M.), and the Osaka Foundation for the Promotion of Clinical Immunology (to M.M.). M.M. and T.H. are listed as inventors in patent applications closely related to results in this paper.

Received: August 30, 2012
Revised: December 4, 2012
Accepted: January 22, 2013
Published: February 21, 2013

REFERENCES

Adachi, Y., Aoki, C., Yoshio-Hoshino, N., Takayama, K., Curiel, D.T., and Nishimoto, N. (2006). Interleukin-6 induces both cell growth and VEGF production in malignant mesotheliomas. Int. J. Cancer *119*, 1303–1311.

Afzali, B., Lombardi, G., Lechler, R.I., and Lord, G.M. (2007). The role of T helper 17 (Th17) and regulatory T cells (Treg) in human organ transplantation and autoimmune disease. Clin. Exp. Immunol. *148*, 32–46.

Arima, Y., Harada, M., Kamimura, D., Park, J.-H., Kawano, F., Yull, F.E., Kawamoto, T., Iwakura, Y., Betz, U.A., Márquez, G., et al. (2012). Regional neural activation defines a gateway for autoreactive T cells to cross the blood-brain barrier. Cell *148*, 447–457.

Atsumi, T., Ishihara, K., Kamimura, D., Ikushima, H., Ohtani, T., Hirota, S., Kobayashi, H., Park, S.J., Saeki, Y., Kitamura, Y., and Hirano, T. (2002). A point mutation of Tyr-759 in interleukin 6 family cytokine receptor subunit gp130 causes autoimmune arthritis. J. Exp. Med. *196*, 979–990.

Awasthi, A., and Kuchroo, V.K. (2009). Th17 cells: from precursors to players in inflammation and infection. Int. Immunol. *21*, 489–498.

Bertram, L., Lill, C.M., and Tanzi, R.E. (2010). The genetics of Alzheimer disease: back to the future. Neuron *68*, 270–281.

Bettelli, E., Oukka, M., and Kuchroo, V.K. (2007). T(H)-17 cells in the circle of immunity and autoimmunity. Nat. Immunol. *8*, 345–350.

Consortium, T.W.T.C.C.; Wellcome Trust Case Control Consortium. (2007). Genome-wide association study of 14,000 cases of seven common diseases and 3,000 shared controls. Nature *447*, 661–678.

Cua, D.J., Sherlock, J., Chen, Y., Murphy, C.A., Joyce, B., Seymour, B., Lucian, L., To, W., Kwan, S., Churakova, T., et al. (2003). Interleukin-23 rather than interleukin-12 is the critical cytokine for autoimmune inflammation of the brain. Nature *421*, 744–748.

D'Acquisto, F., Iuvone, T., Rombolà, L., Sautebin, L., Di Rosa, M., and Carnuccio, R. (1997). Involvement of NF-kappaB in the regulation of cyclooxygenase-2 protein expression in LPS-stimulated J774 macrophages. FEBS Lett. *418*, 175–178.

Ferrand, A., Kowalski-Chauvel, A., Bertrand, C., Escrieut, C., Mathieu, A., Portolan, G., Pradayrol, L., Fourmy, D., Dufresne, M., and Seva, C. (2005). A novel mechanism for JAK2 activation by a G protein-coupled receptor, the CCK2R: implication of this signaling pathway in pancreatic tumor models. J. Biol. Chem. *280*, 10710–10715.

Harrington, L.E., Hatton, R.D., Mangan, P.R., Turner, H., Murphy, T.L., Murphy, K.M., and Weaver, C.T. (2005). Interleukin 17-producing CD4+ effector T cells develop via a lineage distinct from the T helper type 1 and 2 lineages. Nat. Immunol. *6*, 1123–1132.

Hemminki, K., Försti, A., Houlston, R., and Bermejo, J.L. (2011). Searching for the missing heritability of complex diseases. Hum. Mutat. *32*, 259–262.

Hirano, T. (1998). Interleukin 6 and its receptor: ten years later. Int. Rev. Immunol. *16*, 249–284.

Hirano, T. (2010). Interleukin 6 in autoimmune and inflammatory diseases: a personal memoir. Proc. Jpn. Acad. Ser. B Phys. Biol. Sci. *86*, 717–730.

Hirota, K., Hashimoto, M., Yoshitomi, H., Tanaka, S., Nomura, T., Yamaguchi, T., Iwakura, Y., Sakaguchi, N., and Sakaguchi, S. (2007). T cell self-reactivity forms a cytokine milieu for spontaneous development of IL-17+ Th cells that cause autoimmune arthritis. J. Exp. Med. *204*, 41–47.

Igarashi, H., Hashimoto, J., Tomita, T., Yoshikawa, H., and Ishihara, K. (2010). TP53 mutations coincide with the ectopic expression of activation-induced cytidine deaminase in the fibroblast-like synoviocytes derived from a fraction of patients with rheumatoid arthritis. Clin. Exp. Immunol. *161*, 71–80.

Ishihara, K., Sawa, S., Ikushima, H., Hirota, S., Atsumi, T., Kamimura, D., Park, S.J., Murakami, M., Kitamura, Y., Iwakura, Y., and Hirano, T. (2004). The point mutation of tyrosine 759 of the IL-6 family cytokine receptor gp130 synergizes with HTLV-1 pX in promoting rheumatoid arthritis-like arthritis. Int. Immunol. *16*, 455–465.

Iwakura, Y., and Ishigame, H. (2006). The IL-23/IL-17 axis in inflammation. J. Clin. Invest. *116*, 1218–1222.

Jo, E.J., Lee, H.Y., Lee, Y.N., Kim, J.I., Kang, H.K., Park, D.W., Baek, S.H., Kwak, J.Y., and Bae, Y.S. (2004). Group IB secretory phospholipase A2 stimulates CXC chemokine ligand 8 production via ERK and NF-kappa B in human neutrophils. J. Immunol. *173*, 6433–6439.

Johnson, A.D., and O'Donnell, C.J. (2009). An open access database of genome-wide association results. BMC Med. Genet. *10*, 6.

Kaiser, W.J., Upton, J.W., and Mocarski, E.S. (2008). Receptor-interacting protein homotypic interaction motif-dependent control of NF-kappa B activation via the DNA-dependent activator of IFN regulatory factors. J. Immunol. *181*, 6427–6434.

Kim, J., Basak, J.M., and Holtzman, D.M. (2009). The role of apolipoprotein E in Alzheimer's disease. Neuron *63*, 287–303.

Kojima, M., Morisaki, T., Izuhara, K., Uchiyama, A., Matsunari, Y., Katano, M., and Tanaka, M. (2000). Lipopolysaccharide increases cyclo-oxygenase-2 expression in a colon carcinoma cell line through nuclear factor-kappa B activation. Oncogene *19*, 1225–1231.

Lander, E.S. (2011). Initial impact of the sequencing of the human genome. Nature *470*, 187–197.

Maffia, P., Brewer, J.M., Gracie, J.A., Ianaro, A., Leung, B.P., Mitchell, P.J., Smith, K.M., McInnes, I.B., and Garside, P. (2004). Inducing experimental arthritis and breaking self-tolerance to joint-specific antigens with trackable, ovalbumin-specific T cells. J. Immunol. *173*, 151–156.

Manolio, T.A., Collins, F.S., Cox, N.J., Goldstein, D.B., Hindorff, L.A., Hunter, D.J., McCarthy, M.I., Ramos, E.M., Cardon, L.R., Chakravarti, A., et al. (2009). Finding the missing heritability of complex diseases. Nature *461*, 747–753.

Murakami, M., and Hirano, T. (2011). A four step model for the IL-6 amplifier, a regulator of chronic inflammations in tissue-specific MHC class II-associated autoimmune diseases. Front. Immunol. *2*, 22.

Murakami, M., Okuyama, Y., Ogura, H., Asano, S., Arima, Y., Tsuruoka, M., Harada, M., Kanamoto, M., Sawa, Y., Iwakura, Y., et al. (2011). Local

microbleeding facilitates IL-6- and IL-17-dependent arthritis in the absence of tissue antigen recognition by activated T cells. J. Exp. Med. *208*, 103–114.

Nishihara, M., Ogura, H., Ueda, N., Tsuruoka, M., Kitabayashi, C., Tsuji, F., Aono, H., Ishihara, K., Huseby, E., Betz, U.A., et al. (2007). IL-6-gp130-STAT3 in T cells directs the development of IL-17+ Th with a minimum effect on that of Treg in the steady state. Int. Immunol. *19*, 695–702.

Ogura, H., Murakami, M., Okuyama, Y., Tsuruoka, M., Kitabayashi, C., Kanamoto, M., Nishihara, M., Iwakura, Y., and Hirano, T. (2008). Interleukin-17 promotes autoimmunity by triggering a positive-feedback loop via interleukin-6 induction. Immunity *29*, 628–636.

Ohtani, T., Ishihara, K., Atsumi, T., Nishida, K., Kaneko, Y., Miyata, T., Itoh, S., Narimatsu, M., Maeda, H., Fukada, T., et al. (2000). Dissection of signaling cascades through gp130 in vivo: reciprocal roles for STAT3- and SHP2-mediated signals in immune responses. Immunity *12*, 95–105.

O'Shea, J.J., Ma, A., and Lipsky, P. (2002). Cytokines and autoimmunity. Nat. Rev. Immunol. *2*, 37–45.

Park, H., Li, Z., Yang, X.O., Chang, S.H., Nurieva, R., Wang, Y.H., Wang, Y., Hood, L., Zhu, Z., Tian, Q., and Dong, C. (2005). A distinct lineage of CD4 T cells regulates tissue inflammation by producing interleukin 17. Nat. Immunol. *6*, 1133–1141.

Pickell, L., Tran, P., Leclerc, D., Hiscott, J., and Rozen, R. (2005). Regulatory studies of murine methylenetetrahydrofolate reductase reveal two major promoters and NF-kappaB sensitivity. Biochim. Biophys. Acta *1731*, 104–114.

Rojo, A.I., Salinas, M., Martín, D., Perona, R., and Cuadrado, A. (2004). Regulation of Cu/Zn-superoxide dismutase expression via the phosphatidylinositol 3 kinase/Akt pathway and nuclear factor-kappaB. J. Neurosci. *24*, 7324–7334.

Sakaguchi, S., and Sakaguchi, N. (2005). Animal models of arthritis caused by systemic alteration of the immune system. Curr. Opin. Immunol. *17*, 589–594.

Sawa, S., Kamimura, D., Jin, G.H., Morikawa, H., Kamon, H., Nishihara, M., Ishihara, K., Murakami, M., and Hirano, T. (2006). Autoimmune arthritis associated with mutated interleukin (IL)-6 receptor gp130 is driven by STAT3/IL-7-dependent homeostatic proliferation of CD4+ T cells. J. Exp. Med. *203*, 1459–1470.

Sawa, Y., Arima, Y., Ogura, H., Kitabayashi, C., Jiang, J.J., Fukushima, T., Kamimura, D., Hirano, T., and Murakami, M. (2009). Hepatic interleukin-7 expression regulates T cell responses. Immunity *30*, 447–457.

Schmitz, T., Souil, E., Hervé, R., Nicco, C., Batteux, F., Germain, G., Cabrol, D., Evain-Brion, D., Leroy, M.J., and Méhats, C. (2007). PDE4 inhibition prevents preterm delivery induced by an intrauterine inflammation. J. Immunol. *178*, 1115–1121.

Sewell, G.W., Marks, D.J., and Segal, A.W. (2009). The immunopathogenesis of Crohn's disease: a three-stage model. Curr. Opin. Immunol. *21*, 506–513.

Song, Y.J., Jen, K.Y., Soni, V., Kieff, E., and Cahir-McFarland, E. (2006). IL-1 receptor-associated kinase 1 is critical for latent membrane protein 1-induced p65/RelA serine 536 phosphorylation and NF-kappaB activation. Proc. Natl. Acad. Sci. USA *103*, 2689–2694.

Thomas, R.S., Tymms, M.J., McKinlay, L.H., Shannon, M.F., Seth, A., and Kola, I. (1997). ETS1, NFkappaB and AP1 synergistically transactivate the human GM-CSF promoter. Oncogene *14*, 2845–2855.

Veldhoen, M., Hocking, R.J., Atkins, C.J., Locksley, R.M., and Stockinger, B. (2006). TGFbeta in the context of an inflammatory cytokine milieu supports de novo differentiation of IL-17-producing T cells. Immunity *24*, 179–189.

Wolf, I., Pevzner, V., Kaiser, E., Bernhardt, G., Claudio, E., Siebenlist, U., Förster, R., and Lipp, M. (1998). Downstream activation of a TATA-less promoter by Oct-2, Bob1, and NF-kappaB directs expression of the homing receptor BLR1 to mature B cells. J. Biol. Chem. *273*, 28831–28836.

Yang, J., Benyamin, B., McEvoy, B.P., Gordon, S., Henders, A.K., Nyholt, D.R., Madden, P.A., Heath, A.C., Martin, N.G., Montgomery, G.W., et al. (2010). Common SNPs explain a large proportion of the heritability for human height. Nat. Genet. *42*, 565–569.

Zhang, Y., Fujita, N., Oh-hara, T., Morinaga, Y., Nakagawa, T., Yamada, M., and Tsuruo, T. (1998). Production of interleukin-11 in bone-derived endothelial cells and its role in the formation of osteolytic bone metastasis. Oncogene *16*, 693–703.